Investigation of the Effects of Different Carotenoids on the Absorption and CD Signals of Light Harvesting 1 Complexes

6 AUTHORS, INCLUDING:

Sofia Georgakopoulou
ETH Zurich
16 PUBLICATIONS **359** CITATIONS

SEE PROFILE

Gert Van der Zwan
VU University Amsterdam
107 PUBLICATIONS **2,665** CITATIONS

SEE PROFILE

Robert A. Niederman
Rutgers, The State University of New Jersey
96 PUBLICATIONS **2,496** CITATIONS

SEE PROFILE

Rienk van Grondelle
VU University Amsterdam
647 PUBLICATIONS **23,551** CITATIONS

SEE PROFILE

Investigation of the Effects of Different Carotenoids on the Absorption and CD Signals of Light Harvesting 1 Complexes

Sofia Georgakopoulou,[†] Gert van der Zwan,*,‡ John D. Olsen,§ C. Neil Hunter,§ Robert A. Niederman,‖ and Rienk van Grondelle[†]

Department of Biophysics and Physics of Complex Systems, Vrije Universiteit, 1081 HV Amsterdam, The Netherlands, Department of Analytical Chemistry and Applied Spectroscopy, Vrije Universiteit, 1081 HV Amsterdam, The Netherlands, Robert Hill Institute for Photosynthesis Research, Krebs Institute for Biomolecular Research, Department of Molecular Biology and Biotechnology, University of Sheffield, Sheffield S10 2TN, United Kingdom, and Department of Molecular Biology and Biochemistry, Rutgers, The State University of New Jersey, Piscataway, New Jersey 08854

Absorption and circular dichroism (CD) spectra of light-harvesting (LH)1 complexes from the purple bacteria *Rhodobacter* (*Rba.*) *sphaeroides* and *Rhodospirillum* (*Rsp.*) *rubrum* are presented. The complexes exhibit very low intensity, highly nonconservative, near-infrared (NIR) CD spectra. Absorption and CD spectra from several mutant and reconstituted LH1 complexes, with the carotenoid neurosporene and the precursor phytoene replacing the wild-type (WT) carotenoids, are also examined. The experiments show that the position of the carotenoid bands as well as the bacteriochlorophyll (BChl)/carotenoid ratio affect the NIR CD spectra: bluer bands and larger ratios make the NIR CD signal more conservative. Modeling results that support this finding are presented. This study, combined with the theoretical approach of the companion paper, where modeling of such complexes is presented and discussed in detail, provide a complete explanation of the origin of the nonconservative NIR CD spectra of LH1 and B820.

Introduction

Bacteriochlorophylls (BChl) and carotenoids function as the main light-harvesting pigments of purple bacterial antennae systems. They contain extended networks of alternating single and double bonds, the polyenes, which make them very efficient photoreceptors. In particular, BChl consists of a bacteriochlorin ring, where most of the relevant oscillator strength is located, and a phytol chain.[1,2] It exhibits a main absorption band in the near-infrared (NIR) (around 777 nm) arising from the Q_Y transition; another small band in the visible at around 598 nm is due to the Q_X transition, while the Soret transitions (B_Y and B_X) give rise to a third, very broad band in the blue part of the spectrum (around 390 nm). The latter is likely to mix with other states, like the N, and no clear separation is possible in the absorption spectrum.[3] The Y transitions have a transition dipole moment more or less along the N_B–N_D direction of the bacteriochlorin ring, while the X transition dipole moments are close to the N_A–N_C direction; in all cases, there is a deviation of a few degrees from these directions.[1,3,4]

Carotenoids are long polyenes, with conjugated lengths varying from 8 to 13 double bonds. They contribute to light harvesting by absorbing sunlight in the visible part of the spectrum (generally between 400 and 500 nm), where BChls

are mainly inactive;[5] 25−95% of this light is transferred to BChl *a* chromophores.[6–10] Their broad absorption band originates from transitions to the symmetry-allowed S_2 ($1B_u^+$) singlet excited state.[11] In some cases, a very distinct fine structure is observed, caused by the S_2 state's lower vibrational levels. As shown by Dolan et al.[12] and Georgakopoulou et al.,[13] the carotenoid transition dipole moment in the light-harvesting (LH)2 complex lies along the line that connects the carbons of the conjugated chain situated between the B800 and B850 BChls, rather than stretching along the long axis of the pigment. Carotenoids are also known to be important photo-protectors for the organism by virtue of their ability to quench the BChl excited triplet states and prevent the formation of singlet oxygen that is highly reactive and harmful for the complex.[14,15]

In the purple bacteria, BChls and carotenoids associate very effectively with the LH polypeptides to form LH complexes that capture sunlight and transfer the electronic excitation very efficiently to the reaction center (RC),[16,17] where a charge separation takes place. Nowadays, structures and/or structural models are available for many of the complexes involved in the process described above, although the resolution is not always to the atomic level. The RC from *Blastochloris* (formerly *Rhodopseudomonas* (*Rps.*)) *viridis* was the first membrane protein structure to be determined and was obtained in 1985 at a 3 Å resolution.[18] Since then, the resolution for the RC has been improved significantly and is now known to less than 2 Å.[19–24] The structure of the cytochrome bc_1 complex from bovine heart mitochondria was revealed with a resolution of about 3 Å,[25,26] while the ATPase structure is known to 2.8 Å resolution since 1994.[27] In 1995, Karrasch et al.[28] obtained an 8.5 Å resolution structure for LH1 complexes of *Rhodospirillum*

* Corresponding author. E-mail: zwan@chem.vu.nl.
† Department of Biophysics and Physics of Complex Systems, Vrije Universiteit.
‡ Department of Analytical Chemistry and Applied Spectroscopy, Vrije Universiteit.
§ Robert Hill Institute for Photosynthesis Research, Krebs Institute for Biomolecular Research, Department of Molecular Biology and Biotechnology, University of Sheffield.
‖ Department of Molecular Biology and Biochemistry, Rutgers, The State University of New Jersey.

Effects of Carotenoids on LH1 Complexes

J. Phys. Chem. B, Vol. 110, No. 7, 2006 **3355**

(*Rsp.*) *rubrum* by calculating the projection map of electron microscopy data on two-dimensional crystals; this was subsequently improved upon by Jamieson et al.,[29] who used cryo-EM to produce an 8.5 Å structure of the complete RCLH1 core complex. Structural information on the LH2 and LH1, RCLH1X of *Rhodobacter* (*Rba.*) *sphaeroides* complexes was obtained from cryo-EM results of Walz et al.,[30] which demonstrated that LH2 was nonameric like that of *Rps. acidophila*.[31] The latter complex is known today to 2 Å resolution,[32] and together with the structure of the LH2 from *Rsp. molischianum*, an octamer,[33] we have a thorough insight into the organization of the peripheral antenna. Our understanding of the functionality of these systems improved even further when the long-range order of the LH1−RC complexes was reported for membranes of *Rba. sphaeroides*, where the gene PufX is expressed,[34,35] but LH2 was absent. Recently, Roszak et al. (2003)[36] presented a RCLH1 crystal structure from *Rps. palustris* at 4.8 Å resolution. The publication of the architecture of the native photosynthetic membrane of *Rba. sphaeroides*, as imaged by atomic force microscopy, revealed for the first time how all the earlier data fit together in real life.[37] Short linear arrays of RCLH1X core complexes were surrounded by narrow lanes of LH2 complexes, only 1−2 complexes wide, which provided connections to much larger patches containing LH2 exclusively. The use of LD on the same membrane has taken our understanding of the organization of the bacterial photosynthetic membrane one stage further so that we begin to confidently model the complete chromatophore.[38]

While there have been many advances in understanding the organization of the complexes, our understanding of their spectra has been hampered by the lack of 3D structural information, particularly for LH1 complexes. By using absorption and CD spectroscopy and modeling, we have been able to contemplate a more detailed organization of LH complexes.[39−41] On the basis of the known structures, we have explained several aspects of their absorption and CD spectra, like the origin of the red-shift of the zero crossing in the CD signal with respect to the absorption maximum.[42] Moreover, we have been able to estimate the interaction energy between nearest neighbors in the B850 ring by identifying the high exciton component,[43] the position of which has been debated for many years.[44,45] In this work, we examine LH1 complexes from the bacteria *Rba. sphaeroides* and *Rsp. rubrum* by means of absorption and CD spectroscopy. Wild-type (WT) LH1 membrane complexes of *Rba. sphaeroides* that contain the normal carotenoids spheroidene/spheroidenone and also variants containing neurosporene or phytoene, in addition to detergent-isolated *Rsp. rubrum* WT LH1 that contained either spirilloxanthin or neurosporene, were examined. The carotenoids found in the complexes that are studied in this paper vary in their end groups and their length of conjugation. Their molecular structures can be seen in Figure 1. Spirilloxanthin, the carotenoid of the WT LH1 antenna from *Rsp. rubrum*, has the longest π-electron chain, with 13 conjugated double bonds. Spheroidene and spheroidenone, from the WT LH1 of *Rba. sphaeroides*, are next, with 10 and 11 conjugated double bonds, respectively. Neurosporene has 9 conjugated double bonds and no end groups, and finally, the precursor phytoene is the shortest, with only 3 conjugated double bonds. The aim of this study is to explain the absorption and CD signals of the LH1 complexes and to identify the interactions that influence the formation of these signals. In this manner, we gain an insight into the structure of the more poorly resolved LH1 antennae and a deeper understanding of the role of the different pigments within them.
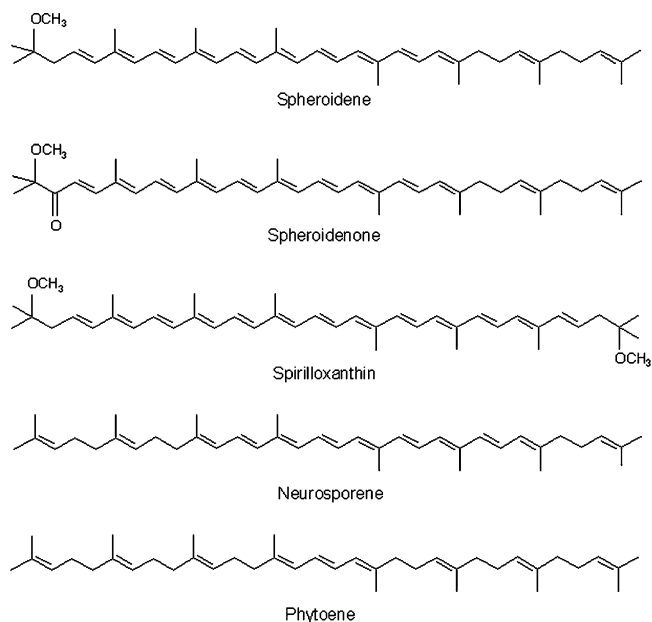

Figure 1. Molecular structures of the carotenoids found in the LH1 complexes presented in this study.

Materials and Methods

Measurements were performed on wild-type (WT) and mutant or reconstituted LH1 complexes from two purple bacteria, namely *Rba. sphaeroides* and *Rsp. rubrum*. Three types of *Rba. sphaeroides* LH1 membrane complexes were used: DD13(RKEK1WT), DD13/DG2(RKEK1WT), and DD13/W(RKEK1WT). These are the LH1-only plasmid, RKEK1WT, complementations of three different carotenoid backgrounds of the double deletion strain DD13 of *Rba. sphaeroides* that does not express any LH or RC complexes.[46] Deletion strain DD13 produces spheroidene and spheroidenone, DD13/DG2 produces mainly neurosporene, and DD13/W produces mainly phytoene. It should be noted that the carotenoid mutants DD13/DG2 and DD13/W are caused by spontaneous, but stable mutations in the carotenoid biosynthetic pathway, which prematurely halt carotenoid synthesis such that either neurosporene or phytoene accumulate in the cell. In the absence of the native carotenoids, spheroidene or spheroidenone, neurosporene or phytoene are incorporated into the LH1 complexes. For the WT membrane complex, a BChl/carotenoid ratio of 1:1 has been measured biochemically. According to the method of preparation and the relative BChl and carotenoid absorption intensities, the neurosporene-containing mutant DG2 is also expected to have a BChl/carotenoid ratio close to 1:1.

For the *Rsp. rubrum* wild-type strain S1, intracytoplasmic membrane vesicles (chromatophores) were first prepared as described in Inamine et al.[47a] Subsequently, the chromatophores were treated with two detergents, lauryl dimethylamine oxide and Triton X-100, and after chromatography on a DEAE-cellulose column, highly purified, stable LH1 complexes, devoid of RCs, were obtained.[48] The pigments in the complex are exclusively BChl *a* and spirilloxanthin, according to a HPLC assay, and the BChl/carotenoid molar ratio is 2:1. For preparation of the neurosporene-containing complex, the LH1 antenna was purified from the carotenoidless *Rsp. rubrum* G9, as described by Miller et al.,[49] except that the gel-filtration step was replaced by isopycnic ultracentrifugation on a 5−25% (w/v) sucrose density gradient, containing 30 mM *n*-octyl β-D-glucopyranoside.[47b] Neurosporene was reconstituted into these purified LH1 complexes by a modification[47b] of the procedure
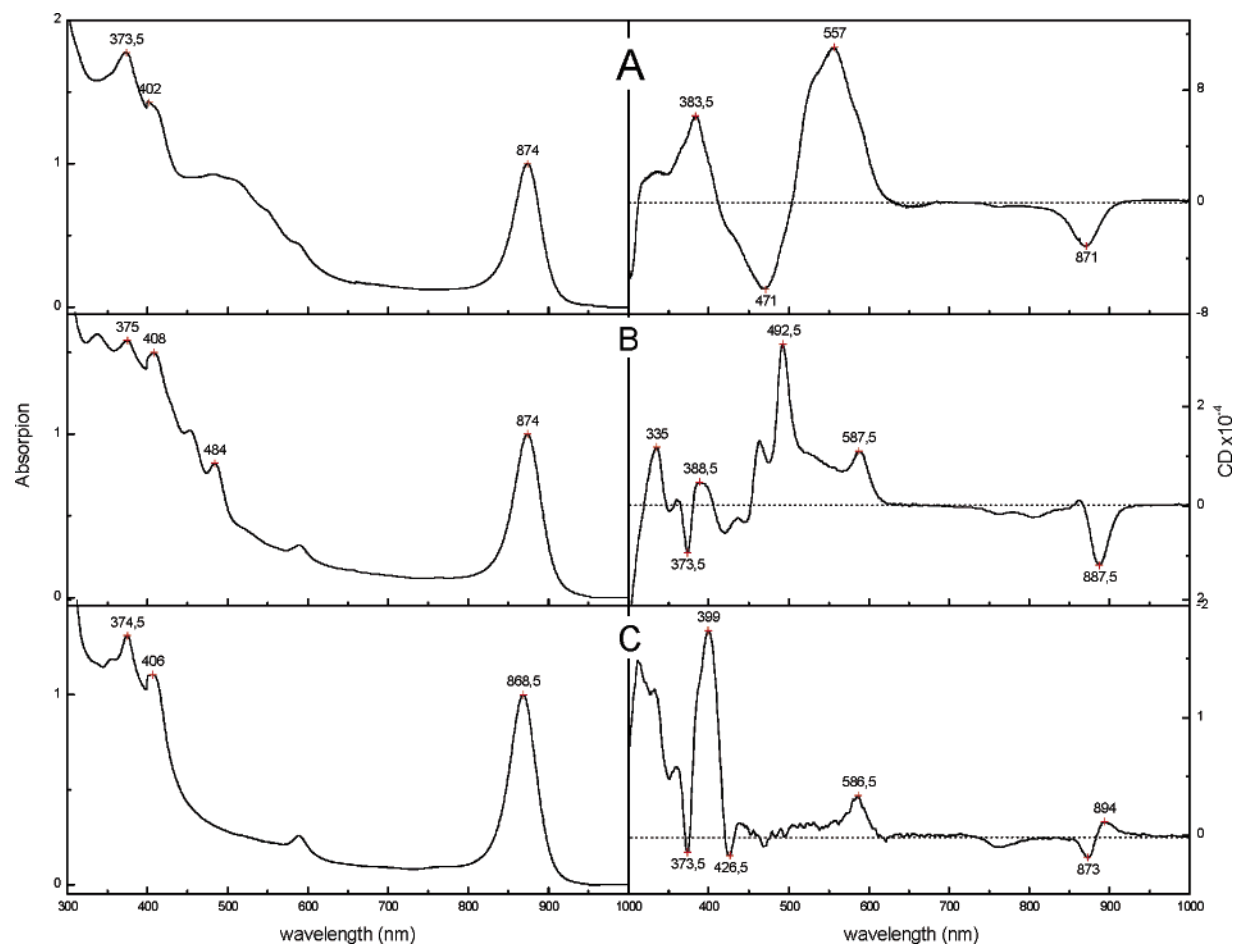
Figure 2. Room temperature (RT) absorption (left) and CD (right) spectra of LH1 complexes in *Rba. sphaeroides* membranes. The absorption spectra are normalized on the Q_Y band, and the CD spectra are subsequently scaled on the normalized absorption. The complexes contain different carotenoids: A, spheroidene and spheroidenone (WT); B, neurosporene; C, phytoene (carotenoid precursor).

of Desamero et al.[50] Complexes prepared in this way have a BChl/carotenoid molar ratio of 3.3:1; this indicates that some carotenoid binding sites are not filled by the reconstitution procedure. The purified B820 complex was prepared from the carotenoidless strain *Rsp. rubrum* G9, as described in Pandit et al.[51] For the room temperature (RT) absorption and CD measurements, complexes were diluted further in 20 mM tricine, pH 7.8, to an optimal maximum OD of approximately 0.5 cm^{-1}. After dilution, the absorption properties remained unchanged, which was a good indication that there is no aggregation of the complexes. For an analysis on the changes that occur to the absorption and CD signals of aggregated complexes, see the companion paper.[52] Triton X-100 (0.1% v/v) was necessary only for preparing the B820 sample. The visible and NIR part of the absorption and CD spectra were measured in a home-built setup described in Georgakopoulou et al.[41] CD spectra in the blue wavelengths were measured with a Jobin-Yvon (Longjumeau, France) CD6 dichrograph, while absorption spectra in that region were recorded with a Specord M 500 spectrophotometer (Zeiss, Germany).

Results

The WT LH1 antennae from *Rba. sphaeroides* and *Rsp. rubrum* exhibit very particular CD spectra, especially in the BChl Q_Y region, where the CD signals are rather small, compared to signals from most LH2 complexes,[40] and highly nonconservative. By changing the carotenoids found in the WT complexes with carotenoids with shorter π-electron chains, we

observe strong effects in the Q_Y region of the CD signal as well as small shifts in the Q_Y absorption.

In particular, for the *Rba. sphaeroides* WT LH1 membrane complex, the Q_Y CD signal is a small negative band with a minimum at 871 nm, 3 nm to the blue of the main absorption maximum (874 nm) (Figure 2A). A much smaller, but distinct negative band can be observed at 763 nm, which, in analogy to our assignment in LH2[43] and according to our modeling results (see below and companion paper[52]), is ascribed to the high exciton component of the Q_Y band. Because of scattering, no bands can be distinguished in the absorption spectrum at this area. The carotenoid bands are very intense, broad, and featureless in both the absorption and CD. Our WT *Rba. sphaeroides* LH1 sample has a BChl/carotenoid ratio of 1:1 and contains a mixture of the carotenoids spheroidene and spheroidenone, which can explain these spectral attributes. The carotenoid absorption band begins toward the red end of the visible spectrum, overlapping with the blue edge of the Q_X band. It has a maximum at 481 nm, and it lies next to the Soret bands that are situated at 400 and 373 nm. The CD signal of the carotenoids has a maximum at 557 nm and a minimum at 471 nm, and it obstructs completely the identification of the Q_X CD. In the Soret, we can distinguish a single positive CD band with a maximum at 383.5 nm. The NIR spectra of this sample have been measured also in low temperature (Figure 3). Upon decrease of the temperature to 77 K, the NIR CD signal becomes slightly more conservative, with a positive feature appearing at the red-most part of the spectrum. The absorption band shifts

Effects of Carotenoids on LH1 Complexes

J. Phys. Chem. B, Vol. 110, No. 7, 2006 **3357**
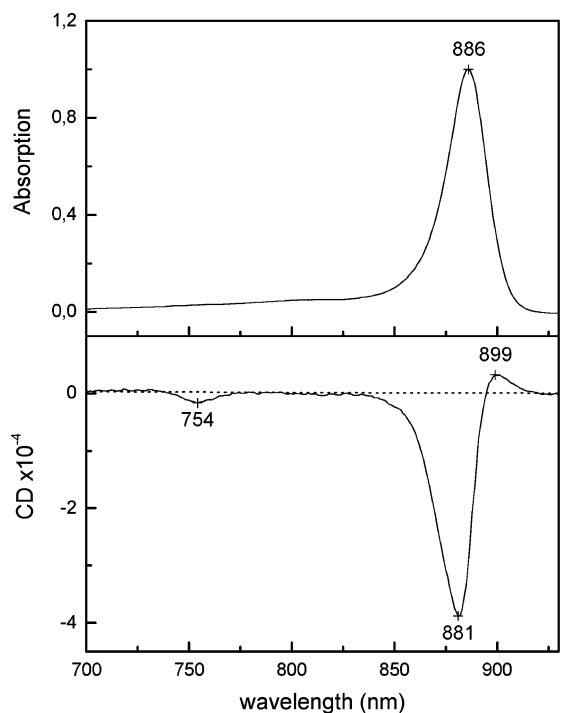
Figure 3. 77 K absorption (top) and CD (bottom) NIR spectra of the LH1 membrane complex from *Rba. sphaeroides*. The absorption spectra are normalized on the Q_Y band and the CD spectra are subsequently scaled on the normalized absorption.

to the red, followed by the CD signal. The scattering in the absorption spectrum is decreased with respect to the RT spectrum; however, it is still difficult to identify with certainty any shoulders. In the CD spectrum, on the other hand, the high exciton band is still clearly visible and has shifted more to the blue, depicting an increase in the size of the excitonic manifold, which could rise as a result of a small shrinkage of the protein and thus an increase of the interaction energy.

When the WT LH1 incorporates neurosporene, the absorption maximum in the Q_Y region remains at 874 nm, but the shape of the CD signal changes significantly (Figure 2B): instead of a single negative peak at 871 nm, we now have a signal with alternating signs, with the minimum near 888 nm and a small maximum at 862 nm. The zero crossing is 6 nm to the blue of the absorption, at 868 nm. Small shoulders are appearing in the blue region of the Q_Y CD, one at 805 nm and another at 761 nm; the latter is very similar to the one distinguished in the WT membrane complex. The Q_X signal is now clearly visible because there is no longer overlap with the carotenoids. The Q_X absorption band is at 589 nm, accompanied with a positive CD signal at the same position. The carotenoid area is now more to the blue and better resolved, with the first absorption maximum situated at 484 nm and the blue edge "merging" into the Soret. In the CD spectrum, it presents a "typical" LH1 carotenoid signal, first observed by Bolt et al.,[53] with two maxima at 492 and 463 nm, followed by two minima at 446 and 421 nm. The next two minima, at 373.5 and 351 nm, belong to the Soret band, which has a main absorption peak at 375 nm. In general, the Q_X and Soret absorption bands of this mutant closely resemble the ones in the WT of *Rba. sphaeroides* and, as we will see next, those of all the other membrane complexes studied. The Soret CD spectrum is, however, much more complicated due to the overlap with the carotenoid bands.

The last membrane complex from *Rba. sphaeroides* is the one containing the carotenoid precursor phytoene. The NIR

absorption maximum of this mutant is shifted to 868.5 nm, while the CD signal is almost fully conservative, with a maximum at 894 nm and a minimum at 873 nm (Figure 2C). A big negative band is situated at 765 nm that corresponds to a shoulder on the absorption, at 763 nm, similar to the other membrane complexes discussed so far. At 589 nm, there is a clear Q_X absorption and the corresponding CD signal is mostly positive, with a maximum at 587 nm. Finally, in the Soret region, there are two absorption peaks at 405 and 374.5 nm and a shoulder at 352 nm. The CD signal has alternating signs, with a main maximum at 400 nm. Note that the signals of phytoene must also lie somewhere hidden in the Soret region; however, they should be relatively small.

The detergent-isolated WT LH1 complex from *Rsp. rubrum* displays a NIR absorption band that is situated at 881 nm. Its corresponding CD signal is nonconservative with a "+ −" signature, which is characteristic of non-native complexes, and it arises as a result of dissociation and reassociation of the complex upon addition of detergent. As we have shown in the past,[54] this non-native CD signal is due to a small rearrangement of the BChls orientation, which, however, does not explain the large nonconservativity. Studies on *Rsp. rubrum* chromatophores[49,55−58] show NIR CD signals that are more conservative. However, chromatophores contain RC, which exhibits large CD signals in the same region as LH1; moreover, the interaction between RC and LH1 is very likely to affect the shape of the entire CD signal in that region. Therefore, such samples cannot be used for our purposes, nor can we safely compare our results with the ones derived from chromatophores. The *Rsp. rubrum* WT LH1 CD signal in the NIR region has a minimum at 867.5 nm (Figure 4A), while there is also a small positive feature at 910 nm. In accordance with the case of *Rba. sphaeroides*, the high exciton band can be distinguished a little further to the blue at 765 nm; moreover, a shoulder is apparent on the blue edge of the main CD signal, at 811 nm. In the absorption spectrum, a shoulder can be identified on the blue wing of the NIR band, at around 770 nm. The carotenoid spectra are also rather red-shifted, with the red edge of the absorption overlapping with the blue edge of the Q_X. In this case, the bands are narrower than the ones exhibited by the LH1 of *Rba. sphaeroides*, and some fine structure can be distinguished. The BChl/carotenoid ratio is 2:1, thus one carotenoid, namely spirilloxanthin, per dimer, similar to the known LH2 structures. The absorption maximum is at 512 nm, while the CD spectrum exhibits small maxima at 556 and 528 nm and minima at 504 and 484 nm. Finally, in the Soret region, the absorption band has a maximum at 376.5 nm and a shoulder at 400 nm, while the CD also exhibits only positive features with a maximum at 366.5 nm.

A neurosporene-containing LH1 complex, prepared by reconstitution of the LH1 antenna from the carotenoidless *Rsp. rubrum* G9, completes the set of LH1 samples that were used for this study (Figure 4B). The NIR absorption of this complex is shifted to 874 nm, 7 nm to the blue compared to the WT LH1. The CD signal in this part of the spectrum is now much more conservative, with a positive and a negative peak, at 892.5 and 857.5, respectively, that have an intensity ratio of 0.75:−1. Again, a very small negative band, the high exciton component, is visible at around 765 nm, corresponding to a shoulder on the blue edge of the main absorption band at 764 nm. The Q_X and Soret bands are very similar to the ones observed in the neurosporene mutant of *Rba. sphaeroides*; in fact, here they are clearer because scattering is not as pronounced. Thus, the Q_X absorption is at 589.5 nm and the corresponding CD signal has a "− +" signature with a broad
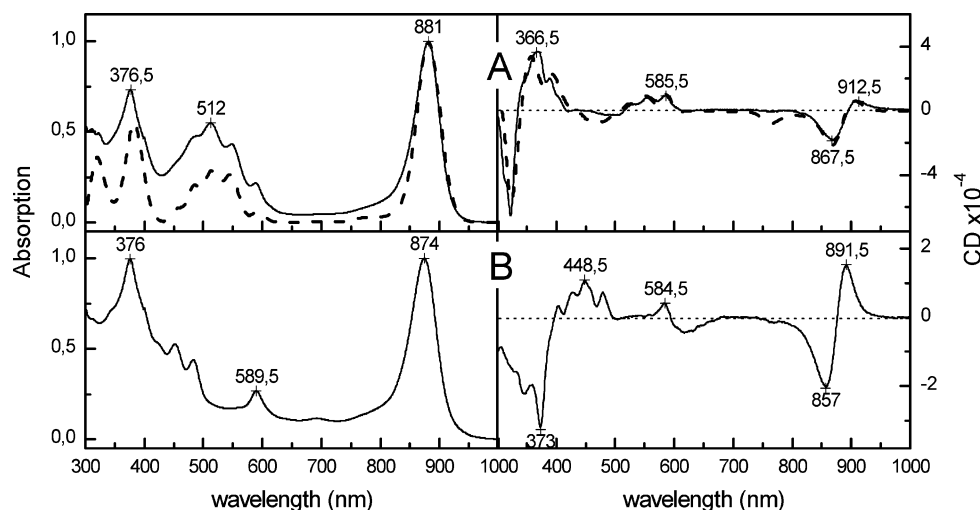
Figure 4. RT absorption (left) and CD (right) spectra of LH1 complexes from *Rsp. rubrum*. The absorption spectra are normalized on the Q_Y band, and the CD spectra are subsequently scaled on the normalized absorption. The complexes contain different carotenoids: A, spirilloxanthin-containing WT LH1 complex isolated by detergent treatment.[46] The calculated spectra are shown by dashed lines, and the modeling parameters are summarized in Table 1. B, carotenoidless LH1 complex isolated by detergent treatment and reconstituted with neurosporene.[47b]

negative feature to the red and a clear positive peak at 584.5 nm. In the Soret, one main absorption peak is distinguished at 376 nm, accompanied by two negative CD signals at 373.5 and 346 nm. As in the other neurosporene mutant, the carotenoid bands of this complex absorb much more to the blue; in particular, the 0−0 absorption peak is at 483 nm. The CD signals are, however, rather different, with the first maximum at 479 nm, followed with a series of positive peaks until the overlap with the Soret region begins. The discrepancy could be explained if we take into account that the BChl/carotenoid ratio in this mutant is 3.3:1, much larger than for all the other complexes.

These rather unusual CD signals led to the need for modeling the absorption and CD spectra and provide some explanation for their origin. Details on the modeling procedure and the relevant results that have led to the final model presented here can be found in the companion paper.[52] Here, we would like to briefly state that the need to take into account the higher transitions of the BChls, as well as the carotenoid transitions, became indispensable in order to achieve a proper fit of the NIR region. From the modeling study, it is concluded that the nonconservative nature of the NIR CD signal is due mainly to the interaction of the BChls with the carotenoids and, to a lesser extent, to the Soret transitions. Rotations of the BChl transition dipole moments can lead to very precise fits between modeling and experiment, as we will see next; however, this is not sufficient to solely explain the appearance of the large nonconservative nature of the signal.

Our results demonstrate that, by including the interactions between all the pigments of the LH1 complex into the excitonic model, we are able to reproduce many of the essential features of the experimental spectra in the calculated ones. To illustrate this point, we present the modeled spectrum of WT LH1 from *Rsp. rubrum*. This complex was chosen because it exhibits less scattering, it has the same BChl/carotenoid ratio as the one assumed in the modeling program (see companion paper),[52] and it still displays a considerable amount of nonconservativity in its NIR CD signal. As can be seen in Figure 4A, there is excellent agreement between the modeled and measured spectra; in particular, the highly nonconservative NIR CD signal is reproduced successfully. Moreover, the higher excitonic band is prominent at 763 nm, verifying the fact that the small negative band seen for all complexes at around the same position is due to the high exciton component. This feature is the main
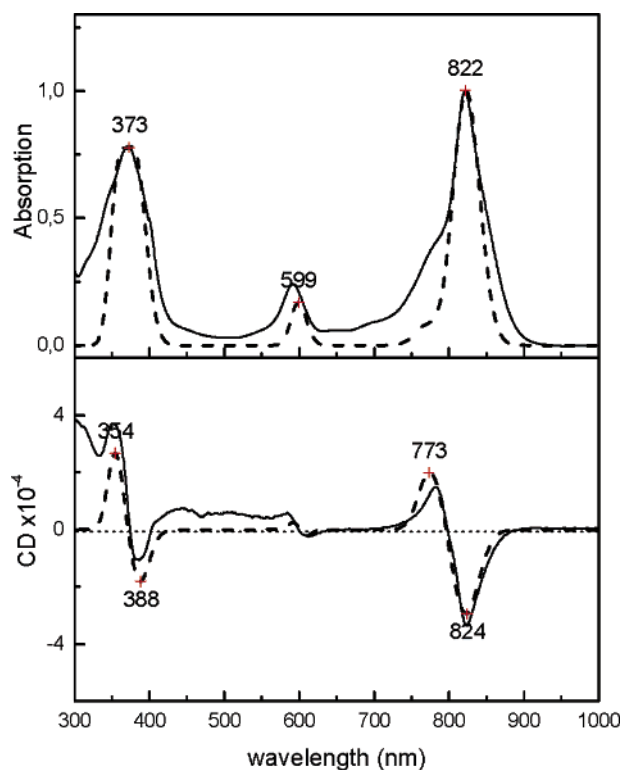
difference between calculated and measured spectra: the modeled high exciton band is much larger than the one observed experimentally. Moreover, a mismatch in the same area can be seen in the absorption spectra, where the model shows a small sideband next to the main absorption band instead of the long blue tail seen in the measured spectrum. The reasons for these discrepancies can be sought in the broadening model used, which is not sufficient to describe features such as high-energy tails in the bands. Here, Gaussians are used to simulate homogeneous broadening; all the excitonic states involved are given the same width (see Table 1) except for the higher one, which is broadened more, to account for its much shorter lifetime.[59] Although broadening the highest state does improve the modeled spectrum, it is still not sufficient to fully account for this discrepancy. By slightly changing the modeling parameters, such as the rotations of the BChl transition dipole moments, it is possible to improve the fit of the modeled high exciton band with the measured one; however, this cannot be done without creating a mismatch at a different part of the spectrum, particularly at the main Q_Y band. The calculated Q_X and carotenoid regions also exhibit striking agreement with the measured spectra, both in the positions and shapes of the bands. Only in the blue-most part of the spectra, below 500 nm, do the differences start to become more prominent due to the uncertainty in the Soret bands and the scattering of the protein. In this case, to improve the model, we added one more state for the BChls, the N state, next to the Soret. The N dipole moment is considered to be along the Y axis, like the B_Y and Q_Y dipole moments. Details on the assigned position and intensity of this band and all the other modeling parameters, including the rotations of the BChl transition moments, can be found in Table 1.

Furthermore, we model the CD and absorption spectra of the B820 complex derived from *Rsp. rubrum* LH1 (Figure 5). The B820 is a LH1 subunit consisting of one dimer of BChl *a* molecules that are excitonically coupled.[60] B820 absorbs at 821 nm, while a distinct shoulder is situated at the blue edge of the absorption, at around 774 nm. This is mostly due to monomeric BChl, small fractions of which are always present in B820 preparations.[61,62] Also very clear are the Q_X band at 591.5 nm and the Soret band at 371.5 nm. The NIR CD signal is nonconservative, with a large negative band at 824 nm and a small positive one at 783 nm. The Q_X also exhibits a "− +"

Effects of Carotenoids on LH1 Complexes

J. Phys. Chem. B, Vol. 110, No. 7, 2006 **3359**

TABLE 1: Parameters Used for the Modeling of the WT LH1 Complex from *Rsp. Rubrum* (Figure 4)

| | BChls | | | | | | | | | | carotenoids | | | |
| | Q_Y | | Q_X | | B_Y | | B_X | | N | | | | | |
	α	β	α	β	α	β	α	β	α	β	0–0	0–1	0–2	0–3
μ (Debye)	6.1	7.3	1.6	2.4	9.5	9.8	−10.7	−10.3	7.5	7.8	6.9	× 1.05	× 0.9	× 0.55
E (nm)	800		594		345		340		335		545	512	483	456
ΔE (cm⁻¹)	350		−30		1330		1510		1330					
ε							1.2							
Δ (cm⁻¹)	500		400				2000				800			
σ (cm⁻¹)	700		600				2100				700			
θ(z) (deg)	−7.2	1.3	−10.0	−10.0	5.0	9.0	−10.0	10.0	5.0	9.0	3.8			

α, β: α-bound and β-bound BChls; 0–0, 0–1, 0–2, 0–3: vibrational levels of the carotenoids; ×: Franck–Condon (FC) factors for the higher vibrational levels, the transition dipole moment of 0–0 is multiplied by the FC factors to give the dipole moments of the higher levels. μ: transition dipole moment; E: site energy; ΔE: energy difference between α- and β-BChls; ε: dielectric constant; Δ: homogeneous broadening; σ: inhomogeneous broadening. θ(z): rotation around the pigment z-axis; for BChls, z-axis is the axis perpendicular to the chlorin ring; for carotenoids, z-axis is the axis perpendicular to the plane defined by the transition dipole moment vector and the long axis of the carotenoid; minus sign denotes anticlockwise rotation.

Figure 5. Modeled absorption (top) and CD (bottom) spectra of B820. In dotted lines, the measured spectra are overlaid. The absorption spectra are normalized on the Q_Y band and the CD spectra are subsequently scaled on the normalized absorption.

TABLE 2: Parameters Used for the Modeling of the B820 Complex (Figure 5)[a]

| | Q_Y | | Q_X | | B_Y | | B_X | |
	α	β	α	β	α	β	α	β
μ (Debye)	6.1	7.3	2.6	3.4	9.5	9.8	−10.7	−10.3
E (nm)	796		600		370		370	
ΔE (cm⁻¹)	350		−30		1330		1510	
ε				1.5				
Δ (cm⁻¹)	400		300		2000		2000	
σ (cm⁻¹)	600		400		2100		2100	
θ(z) (deg)	0.0	4.0	15.0	15.0	7.0	7.0	10.0	10.0

[a] Symbols denote the same parameters as in Table 1.

NIR CD signals from carotenoid-less LH1 mutants (i.e., as in a recent study by Lupo and Gosh[63]) to interactions with higher BChl transitions.[64] However, it is not possible to produce completely negative signals based solely on the interaction of the BChl Q_Y transitions with the Soret. The need to take more interactions into account, the ones in the visible part of the spectrum, is clearly evident.

Discussion and Conclusions

This paper is part of an extensive study of the spectroscopic characteristics of LH1 complexes and the interactions between the pigments that form these complexes. In particular, by using their absorption and CD signals, we try to extrapolate from the known LH2 structures to the structure of the LH1 antennae. Furthermore, we investigate the relations between BChls and carotenoids, first experimentally, in this paper, by measuring the absorption and CD spectra of complexes with different carotenoids, and then, theoretically, by trying to reproduce these signals and identify the interactions that are indispensable for the success of the calculations. The majority of the calculations are presented and explained in the companion paper;[52] here, we give a few examples that demonstrate the importance of incorporating higher transitions and their effect on the NIR signals. Most importantly, they prove that excitonic interactions are dominating these spectra and that the known LH2 structures can be used as a basis for successfully reproducing the experimental results.

The first conclusion we can draw by looking at the experimental spectra is that, by introducing different carotenoids into the complexes, we influence not only the green-blue part of the spectrum, but also the NIR. In particular, looking at each bacterial species separately, we notice that the Q_Y region is greatly affected by the position of the carotenoid bands. Redder absorbing carotenoids distort the conservative nature of the Q_Y

signature at 612 and 584.5 nm, respectively. The same is observed for the Soret CD signal, with a minimum at 386 nm and a maximum at 352.5 nm. By using the parameters listed in Table 2, we can achieve very good agreement between the modeled and measured absorption and CD spectra (Figure 5), with all the important features of the measured signals reproduced. In the NIR region, the absorption has a maximum at 822 nm, and a wide shoulder on its blue side, specifically at 772 nm, the high exciton band. The calculated NIR CD signal has the same signature, and it is nonconservative to approximately the same degree as the measured CD signal. For reproducing the blue-most part of the spectra in this case, only the Soret bands are taken into account. These results show that the Soret transitions can affect the shape of the Q_Y CD bands to a certain extent, causing them to become nonconservative. It is, therefore, possible to ascribe the nonconservativity of the

CD signal significantly, rendering it almost completely non-conservative when the carotenoid transitions lie immediately adjacent to the Q_X band. Carotenoids that do not actually bind to the complex will have a very small effect on the CD spectra because the CD signals of free carotenoids are much smaller than their excitonic CD signal in a LH complex.[41] The Q_Y absorption bands are also affected, although the changes are less significant and are demonstrated by shifts to the red of a few nanometers.

Looking at all the complexes measured, we can also evaluate the effect of the carotenoid content on the BChl Q_Y signal. It is clear that complexes with lower BChl/carotenoid ratios demonstrate larger effects on the Q_Y region. Thus, the completely negative NIR CD signal belongs to the LH1 complex with the lowest BChl/carotenoid ratio, namely the LH1 of *Rba. sphaeroides* WT, with a ratio of 1:1. The neurosporene-containing LH1 from *Rsp. rubrum*, with a ratio of 3.3:1, has the most conservative NIR CD, excluding, of course, the phytoene mutant from *Rba. sphaeroides*, because phytoene is a precursor carotenoid with a very limited conjugated bond system and it absorbs far to the blue.

In the LH2 complexes studied in the past,[41,40] we do not observe such a strong loss of the conservative nature of the Q_Y CD signal for various carotenoid-containing complexes. The NIR CD signal of those LH2 complexes is much more intense than the one of the LH1s studied here, and this can render the carotenoid effect unnoticeable. In addition, the carotenoid bands in the LH2 complexes presented in the previous studies are more blue-shifted than those in the WT LH1s studied here, therefore, the interaction with the Q_Y is smaller and the effects are not expected to be very strong, as discussed earlier in this section. It is likely that the nonconservative nature of the B800 CD band in LH2 is due not only to the effect of the B850 high exciton component, but also to interaction with carotenoids; furthermore, the slight nonconservative nature of the B850 CD band can also be attributed to the interaction with the carotenoids.

At this point, we would like to point out that the changes observed in the CD signals at the Q_Y region are not necessarily caused solely by the carotenoid−BChl interactions, or generally by the interactions with higher states. The effect may be enhanced by other causes, such as high-order structural changes (changes in the shape of the rings)[36−38,65,66] or variations in the protein environment of the pigments. However, our experimental results show that some of the effect must be due to the aforementioned interactions, and this conclusion is supported by theoretical calculations in the companion paper. In the latter, certain structural deviations from the circular structure are examined, an example of modeling of an open ring is given. Moreover, deviations from the circular structure to an ellipse have been examined in a past paper where absorption and CD spectra from rings of carotenoids are calculated.[41] The effect of such changes has so far proven to be small; however, we cannot discard the possibility that they play a role in the formation of the CD spectra of these LH1 complexes.

In conclusion, we would like once again to highlight the importance of the BChl−carotenoid interactions on the BChl Q_Y CD signals. The effect becomes very clear in the light of the set of experimental results presented in this study. The WT CD signals of the LH1 from *Rba. sphaeroides* and *Rsp. rubrum* are very low in intensity and highly nonconservative; this is the result of the interaction with the carotenoids, and its effect is very pronounced because the intensity of the CD signals is relatively small. When the interaction with the carotenoids weakens, either because the carotenoids have shorter conjugated

bond systems and are more blue-shifted, or because the BChl/carotenoid ratio is smaller, the Q_Y CD signal becomes more conservative. The theoretical calculations presented in the companion paper strongly support this conclusion.

References and Notes

(1) Budzikiewicz, H. In *The Porphyrins*; Dolphin, D., Ed.; Academic Press: New York, San Francisco, London, 1978; Vol. III, pp 395−461.

(2) Scheer, H. In *Chlorophylls*; Scheer, H. Ed.; CRC Press: Boca Raton, 1991; pp 3−30.

(3) Weiss, C. In *The Porphyrins*; Dolphin, D., Ed.; Academic Press: New York, San Francisco, London, 1978; Vol. III, pp 211−223.

(4) Scherz, A.; Rosenbach-Belkin, V.; Fisher, J. R. E. In *Chlorophylls*; Scheer, H., Ed.; CRC Press: Boca Raton, 1991; pp 237−268.

(5) Britton, G. In *Carotenoids*; Britton, G., Liaaen-Jensen, S., Pfander, H., Eds.; Birkhäuser: Basel, Boston, Berlin, 1995; Vol. 1B (Spectroscopy), pp 13−62.

(6) Andersson, P. O.; Cogdell, R. J.; Gillbro, T. *Chem. Phys.* **1996**, *210*, 195−217.

(7) Chadwick, B. W.; Zhang, C. Y.; Cogdell, R. J.; Frank, H. A. *Biochim. Biophys. Acta* **1987**, *893*, 444−451.

(8) Kramer, H. J. M.; van Grondelle, R.; Hunter, C. N.; Westerhuis, W. H. J.; Amesz, J. *Biochim. Biophys. Acta* **1984**, *765*, 156.

(9) Mimuro, M.; Katoh, T. *Pure Appl. Chem.* **1991**, *63*, 123−130.

(10) Scholes, G. D.; Harcourt, R. D.; Fleming, G. R. *J. Phys. Chem. B* **1997**, *101*, 7302−7312.

(11) Ritz, T.; Damjanovic, A.; Schulten, K.; Zhang, J. P.; Koyama, Y. *Photosynth. Res.* **2000**, *66*, 125−144.

(12) Dolan, P. M.; Miller, D.; Cogdell, R. J.; Birge, R. R.; Frank, H. A. *J. Phys. Chem. B* **2001**, *105*, 12134−12142.

(13) Georgakopoulou, S.; Cogdell, R. J.; van Grondelle, R.; van Amerongen, H. *J. Phys. Chem. B* **2003**, *107*, 655−658.

(14) Cogdell, R. J.; Frank, H. A. *Biochim. Biophys. Acta* **1987**, *895*, 63−79.

(15) Nilsson, R.; Merkel, P. B.; Kearns, D. R. *Photochem. Photobiol.* **1972**, *16*, 117−124.

(16) van Grondelle, R.; Dekker: J. P.; Gillbro, T.; Sundström, V. *Biochim. Biophys. Acta* **1994**, *1187*, 1−65.

(17) Dutton, P. L.; Prince, R. C. In *The Photosynthetic Bacteria*; Clayton, R. K., Sistrom, W. S., Eds.; Plenum Press: New York, 1978; pp 525−570.

(18) Deisenhofer, J.; Epp, O.; Miki, K.; Huber, R.; Michel, H. *Nature* **1985**, *318*, 618−624.

(19) Katona, G.; Andreasson, U.; Landau, E. M.; Andreasson, L. E.; Neutze, R. *J. Mol. Biol.* **2003**, *331*, 681−692.

(20) Arnoux, B.; Gaucher, J. F.; Ducruix, A.; Reisshusson, F. *Acta Crystallogr., Sect. D* **1995**, *51*, 368−379.

(21) Deisenhofer, J.; Epp, O.; Sinning, I.; Michel, H. *J. Mol. Biol.* **1995**, *246*, 429−457.

(22) Ermler, U.; Fritzsch, G.; Buchanan, S. K.; Michel, H. *Structure* **1994**, *2*, 925−936.

(23) Chang, C. H.; Elkabbani, O.; Tiede, D.; Norris, J.; Schiffer, M. *Biochemistry* **1991**, *30*, 5352−5360.

(24) Fritzsch, G.; Koepke, J.; Diem, R.; Kuglstatter, A.; Baciou, L. *Acta Crystallogr., Sect. D* **2002**, *58*, 1660−1663.

(25) Xia, D.; Yu, C. A.; Kim, H.; Xian, J. Z.; Kachurin, A. M.; Zhang, L.; Yu, L.; Deisenhofer, J. *Science* **1997**, *277*, 60−66.

(26) Iwata, S.; Lee, J. W.; Okada, K.; Lee, J. K.; Iwata, M.; Rasmussen, B.; Link, T. A.; Ramaswamy, S.; Jap, B. K. *Science* **1998**, *281*, 64−71.

(27) Abrahams, J. P.; Leslie, A. G. W.; Lutter, R.; Walker, J. E. *Nature* **1994**, *370*, 621−628.

(28) Karrasch, S.; Bullough, P. A.; Ghosh, R. *EMBO J.* **1995**, *14*, 631−638.

(29) Jamieson, S. J.; Wang, P. Y.; Qian, P.; Kirkland, J. Y.; Conroy, M. J.; Hunter, C. N.; Bullough, P. A. *EMBO J.* **2002**, *21*, 3927−3935.

(30) Walz, T.; Jamieson, S. J.; Bowers, C. M.; Bullough, P. A.; Hunter, C. N. *J. Mol. Biol.* **1998**, *282*, 833−845.

(31) McDermott, G.; Prince, S. M.; Freer, A. A.; Hawthornthwaite-Lawless, A. M.; Papiz, M. Z.; Cogdell, R. J.; Isaacs, N. W. *Nature* **1995**, *374*, 517−521.

(32) Papiz, M. Z.; Prince, S. M.; Howard, T. D.; Cogdell, R. J.; Isaacs, N. W. *J. Mol. Biol.* **2003**, *326*, 1523−1538.

(33) Koepke, J.; Hu, X. C.; Muenke, C.; Schulten, K.; Michel, H. *Structure* **1996**, *4*, 581−597.

(34) Jungas, C.; Ranck, J. L.; Rigaud, J. L.; Joliot, P.; Vermeglio, A. *EMBO J.* **1999**, *18*, 534−542.

Effects of Carotenoids on LH1 Complexes

J. Phys. Chem. B, Vol. 110, No. 7, 2006 **3361**

(35) Frese, R. N.; Olsen, J. D.; Branvall, R.; Westerhuis, W. H. J.; Hunter, C. N.; van Grondelle, R. *Proc. Natl. Acad. Sci. U.S.A.* **2000**, *97*, 5197−5202.

(36) Roszak, A. W.; Howard, T. D.; Southall, J.; Gardiner, A. T.; Law, C. J.; Isaacs, N. W.; Cogdell, R. J. *Science* **2003**, *302*, 1969−1972.

(37) Bahatyrova, S.; Frese, R. N.; Siebert, C. A.; Olsen, J. D.; van der Werf, K. O.; van Grondelle, R.; Niederman, R. A.; Bullough, P. A.; Otto, C.; Hunter, C. N. *Nature* **2004**, *430*, 1058−1062.

(38) Frese, R. N.; Siebert, C. A.; Niederman, R. A.; Hunter, C. N.; Cees, O.; van Grondelle, R. *Proc. Natl. Acad. Sci. U.S.A.* **2004**, *101*, 17994−17999.

(39) Koolhaas, M. H. C.; van der Zwan, G.; van Mourik, F.; van Grondelle, R. *Biophys. J.* **1997**, *72*, 1828−1841.

(40) Georgakopoulou, S.; Frese, R. N.; Johnson, E.; Koolhaas, M. H. C.; Cogdell, R. J.; van Grondelle, R.; van der Zwan, G. *Biophys. J.* **2002**, *82*, 2184−2197.

(41) Georgakopoulou, S.; van Grondelle, R.; van der Zwan, G. *Biophys. J.* **2004**, *87*, 3010−3022.

(42) Koolhaas, M. H. C.; van der Zwan, G.; Frese, R. N.; van Grondelle, R. *J. Phys. Chem. B* **1997**, *101*, 7262−7270.

(43) Koolhaas, M. H. C.; Frese, R. N.; Fowler, G. J. S.; Bibby, T. S.; Georgakopoulou, S.; van der Zwan, G.; Hunter, C. N.; van Grondelle, R. *Biochemistry* **1998**, *37*, 4693−4698.

(44) Wu, H. M.; Ratsep, M.; Lee, I. J.; Cogdell, R. J.; Small, G. J. *J. Phys. Chem. B* **1997**, *101*, 7654−7663.

(45) Wu, H. M.; Savikhin, S.; Reddy, N. R. S.; Jankowiak, R.; Cogdell, R. J.; Struve, W. S.; Small, G. J. *J. Phys. Chem.* **1996**, *100*, 12022−12033.

(46) Jones, M. R.; Fowler, G. J. S.; Gibson, L. C. D.; Grief, G. G.; Olsen, J. D.; Crielaard, W.; Hunter, C. N. *Mol. Microbiol.* **1992**, *6*, 1173−1184.

(47) (a) Inamine, G. S.; Niederman, R. A. *J. Bacteriol.* **1982**, *150*, 1145−1153. (b) Shih, J. D.; Breitbart, S. I.; Niederman, R. A. *The Rutgers Scholar* **2003**, *5*, (http://rutgersscholar.rutgers.edu/volume05/shih-breitbart-neiderman/shih-breitbart-neiderman.htm).

(48) Picorel, R.; Bélanger, G.; Gingras, G. *Biochemistry* **1983**, *22*, 2491−2497.

(49) Miller, J. F.; Hinchigeri, S. B.; Parkes-Loach, P. S.; Callahan, P. M.; Sprinkle, J. R.; Riccobono, J. R.; Loach, P. A. *Biochemistry* **1987**, *26*, 5055−5062.

(50) Desamero, R. Z. B.; Chynwat, V.; van der Hoef, I.; Jansen, F. J.; Lugtenburg, J.; Gosztola, D.; Wasielewski, M. R.; Cua, A.; Bocian, D. F.; Frank, H. A. *J. Phys. Chem. B* **1998**, *102*, 8151−8162.

(51) Pandit, A.; Visschers, R. W.; van Stokkum, I. H. M.; Kraayenhof, R.; van Grondelle, R. *Biochemistry* **2001**, *40*, 12913−12924.

(52) Georgakopoulou, S.; van Grondelle, R.; van der Zwan, G. *J. Phys. Chem. B* **2006**, *110*, 3344−3353.

(53) Bolt, J. D.; Hunter, C. N.; Niederman, R. A.; Sauer, K. *Photochem. Photobiol.* **1981**, *34*, 653−656.

(54) Pandit, A.; van Stokkum, I. H. M.; Georgakopoulou, S.; van der Zwan, G.; van Grondelle, R. *Photosynth. Res.* **2003**, *75*, 235−248.

(55) Qian, P.; Addlesee, H. A.; Ruban, A. V.; Wang, P.; Bullough, P. A.; Hunter, C. N. *J. Biol. Chem.* **2003**, *278*, 23678−23685.

(56) Chang, M. C.; Callahan, P. M.; Parkes-Loach, P. S.; Cotton, T. M.; Loach, P. A. *Biochemistry* **1990**, *29*, 421−429.

(57) Cogdell, R. J.; Scheer, H. *Photochem. Photobiol.* **1985**, *42*, 669−678.

(58) Davis, C. M.; Bustamante, P. L.; Loach, P. A. *J. Biol. Chem.* **1995**, *270*, 5793−5804.

(59) Novoderezhkin, V.; van Grondelle, R. *J. Phys. Chem. B* **2002**, *106*, 6025−6037.

(60) van Mourik, F.; van der Oord, C. J. R.; Visscher, K. J.; Parkes-Loach, P. S.; Loach, P. A.; Visschers, R. W.; Van Grondelle, R. *Biochim. Biophys. Acta* **1991**, *1059*, 111−119.

(61) Parkes-Loach, P. S.; Sprinkle, J. R.; Loach, P. A. *Biochemistry* **1988**, *27*, 7, 2718−2727.

(62) Visschers, R. W.; Nunn, R.; Calkoen, F.; van Mourik, F.; Hunter, C. N.; Rice, D. W.; van Grondelle, R. *Biochim. Biophys. Acta* **1992**, *1100*, 259−266.

(63) Lupo, D.; Ghosh, R. *J. Bacteriol.* **2004**, *186*, 5585−5595.

(64) Koolhaas, M. H. C.; van der Zwan, G.; van Mourik, F.; van Grondelle, R. *Biophys. J.* **1997**, *72*, 1828−1841.

(65) Scheuring, S.; Levy, D.; Rigaud, J. L. *Biochim. Biophys. Acta* **2005**, *1712*, 109−127.

(66) Bahatyrova, S.; Frese, R. N.; van der Werf, K. O.; Otto, C.; Hunter, C. N.; Olsen, J. D. *J. Biol. Chem.* **2004**, M313039200.